



Structure based discovery of novel hexokinase 2 inhibitors

Yang Liu^{a,1}, Mingxue Li^{a,1}, Yujie Zhang^{a,1}, Canrong Wu^b, Kaiyin Yang^b, Suyu Gao^a, Mengzhu Zheng^{b,*}, Xingzhou Li^{c,*}, Hua Li^{a,b,*}, Lixia Chen^{a,*}

^a Wuya College of Innovation, Key Laboratory of Structure-Based Drug Design & Discovery, Ministry of Education, Shenyang Pharmaceutical University, Shenyang 110016, China

^b Hubei Key Laboratory of Natural Medicinal Chemistry and Resource Evaluation, School of Pharmacy, Tongji Medical College, Huazhong University of Science and Technology, Wuhan 430030, China

^c National Engineering Research Center for the Emergency Drug, Beijing Institute of Pharmacology and Toxicology, Beijing 100850, China

ARTICLE INFO

Keywords:

Cancer metabolism
Drug discovery
HK2 inhibitors
Structure-based virtual ligand screening

ABSTRACT

Hexokinase 2 (HK2) is over-expressed in most of human cancers and has been proved to be a promising target for cancer therapy. In this study, based on the structure of HK2, we screened over 6 millions of compounds to obtain the lead. A total of 26 (*E*)-*N'*-(2,3,4-trihydroxybenzylidene) arylhydrazide derivatives were then designed, synthesized, and evaluated for their HK2 enzyme activity and IC₅₀ values against two cancer cell lines. Most of the 26 target compounds showed excellently *in vitro* activity. Among them, compound **3j** showed the strongest inhibitory effects on HK2 enzyme activity with an IC₅₀ of 0.53 ± 0.13 μM and exhibited the most potent growth inhibition against SW480 cells with an IC₅₀ of 7.13 ± 1.12 μM, which deserves further studies.

1. Introduction

In the 1920s, Otto Warburg demonstrated that the energy metabolism pattern of tumor cells was different from that of the normal tissue cells. Normal tissues mainly produce energy through oxidative phosphorylation in the mitochondria, while tumor cells mainly rely on aerobic glycolysis to meet the metabolic needs of cell proliferation [1]. The glycolytic pathway involves a variety of key enzymes, including glucose transporter (GLUT), hexokinase (HK), phosphoric acid fructose kinase (PFK) [2], pyruvate kinase (PK) [3] and lactate dehydrogenase (LDH) [4]. The inhibition of these key metabolic proteins can stem the energy supply to tumor cells, thus inhibiting cell growth [1]. Among the 4 hexokinase isomers (HK1-4), HK2 has a distinct expression pattern, where it is not expressed in most normal tissues, but is overexpressed in more than 70% of cancer cells [5]. This suggests that specific targeting of HK2 may be a good treatment strategy to suppress cancer cell growth by inhibiting glycolysis [6]. Hexokinase 2 (HK2) catalyzes the irreversible first step of the glycolytic pathway, namely, converting glucose into glucose-6-phosphate (G6P) [7]. The inhibition of HK2 can reduce the production of ATP in cancer cells, decrease the carbon supply from glycolysis to the carboxylic acid (TCA) cycle, and decrease the synthesis of nucleotides and fatty acids [8], all of which culminate in the death of

cancer cells [9–11].

Although HK2 has been a potential target for cancer treatment for many years, several challenges still remain in the discovery and design of efficient and selective HK2 inhibitors. These challenges are arise out of the structural properties of HK2, including the high polarity of the active site of the enzyme and the difficulty in specifically inhibiting the different isoenzymes. Therefore, there is still no potent and selective HK2 inhibitor in clinical use thus far [12]. Metformin, 2-deoxyglucose, and 3-bromopyruvate are the most commonly reported HK2 inhibitors [13–15]. However, there are shortcomings with each of these compounds that prevent them from being developed as viable HK2 inhibitors. For example, metformin shows only a weak antitumor activity *in vivo* and *in vitro* [16]. The antitumor potency of 2-deoxyglucose is also weak, and only evident at non-physiologic concentrations [17]. There are adverse effects associated with the use of 3-bromopyruvate because of its off-target effects. The compound also has a short half-life [18]. Therefore, discovering more effective, selective, and less toxic HK2 inhibitors remains a significant challenge to the development of cancer therapies [19].

In our previous study, structure-based virtual ligand screening was adopted to screen the FDA-approved drug database, and Benserazide, a peripherally acting DOPA decarboxylase inhibitor used to treat

* Corresponding authors at: Wuya College of Innovation, Key Laboratory of Structure-Based Drug Design & Discovery, Ministry of Education, Shenyang Pharmaceutical University, Shenyang 110016, China (H. Li).

E-mail addresses: mengzhu_zheng@hust.edu.cn (M. Zheng), xingzhouli@aliyun.com (X. Li), li_hua@hust.edu.cn (H. Li), syzclx@163.com (L. Chen).

¹ These authors contributed equally to this work.

<https://doi.org/10.1016/j.bioorg.2020.103609>

Received 5 December 2019; Received in revised form 19 January 2020; Accepted 20 January 2020

Available online 21 January 2020

0045-2068/ © 2020 Elsevier Inc. All rights reserved.

Parkinson's disease, was identified as an HK2 inhibitor [20]. Encouraged by this finding, ZINC lead-like compound library with 6,053,287 molecules was further screened, which led to the discovery of a new scaffold of HK2 inhibitors [21]. A novel scaffold of (*E*)-*N'*-(2,3,4-trihydroxybenzylidene) arylhydrazide was identified as the lead compound. A series of novel HK2 inhibitors were then designed and synthesized based on the structure of the lead compound. Among them, compound **3j** displayed the strongest potency in inhibiting HK2 enzyme activity and the proliferation of cancer cells.

2. Experiment

2.1. Chemistry

All reactions were carried out in flame-dried glassware under an atmosphere of argon, all reagents were procured from commercial sources (purity > 99%) and used without further purification. Silica gel GF254 and silica gel (200–300 mesh) were respectively used for thin-layer chromatography and column chromatography. NMR spectra were recorded on a Bruker AM-400 spectrometer, with ¹H and ¹³C NMR chemical shifts referenced to the solvent or solvent impurity peaks for DMSO-*d*₆ (δ_{H} 2.50 and δ_{C} 39.52). HRESIMS data were acquired using a Thermo Fisher LC-LTQ-Orbitrap XL spectrometer and an electrospray ionization and a hybrid quadrupole time-of-flight (q-TOF) mass spectrometer (model 6540, Agilent). All other common chemicals, solvents and reagents were of highest grade available from various commercial sources.

2.1.1. General procedure for the synthesis of hydrazides **2**

Hydrazine hydrate (5 mL, 40%) was added to a solution of required ester (5.0 mmol) in methanol (20 mL). The solution was refluxed for 12–24 h and monitored by TLC until starting material was completely consumed. After that, solvent was evaporated under reduced pressure and a small amount of water (5 mL) was added to precipitate the hydrazide, which was filtered and dried in vacuum to give a shiny white to yellow solid in excellent yields, without further purification.

2.1.2. General procedure for the synthesis of hydrazides **3a–3z**

2,3,4-Trihydroxybenzaldehyde (0.55 g, 3.6 mmol) was added to a solution of hydrazides (3.0 mmol) in methanol (20 mL). The solution was stirred for 12 h under room temperature, which was then filtered and finally recrystallized from ethanol, to give the target hydrazone derivatives as white to gray powdered solid.

2.1.3. (*E*)-*N'*-(2,3,4-trihydroxybenzylidene)quinoline-2-carbohydrazide (**3a**)

Yield 72.1%. ¹H NMR (400 MHz, DMSO-*d*₆) δ 12.42 (s, 1H), 11.62 (s, 1H), 9.58 (s, 1H), 8.77 (s, 1H), 8.62 (d, *J* = 8.5 Hz, 1H), 8.57 (brs, 1H), 8.24–8.21 (m, 2H), 8.11 (d, *J* = 7.8 Hz, 1H), 7.94–7.90 (m, 1H), 7.78–7.74 (m, 1H), 6.80 (d, *J* = 8.5 Hz, 1H), 6.44 (d, *J* = 8.0 Hz, 1H); ¹³C NMR (100 MHz, DMSO-*d*₆) δ 160.7, 152.3, 149.9, 149.4, 148.1, 146.5, 138.5, 133.2, 131.2, 129.6, 129.4, 128.8, 128.6, 121.9, 119.5, 111.3, 108.22. HRMS (ESI) *m/z* 324.0981 [M + H]⁺ (calcd for C₁₇H₁₄N₃O₄, 324.0984).

2.1.4. (*E*)-4-(2-hydroxyethoxy)-*N'*-(2,3,4-trihydroxybenzylidene)benzohydrazide (**3b**)

Yield 70.9%. ¹H NMR (400 MHz, DMSO-*d*₆) δ 11.86 (s, 1H), 11.61 (s, 1H), 9.49 (s, 1H), 8.51 (s, 1H), 8.44 (s, 1H), 7.90 (d, *J* = 8.8 Hz, 2H), 7.08 (d, *J* = 8.9 Hz, 2H), 6.77 (d, *J* = 8.5 Hz, 1H), 6.40 (d, *J* = 8.0 Hz, 1H), 4.95 (brs, 1H), 4.08 (t, *J* = 4.9 Hz, 2H), 3.75 (t, *J* = 4.8 Hz, 2H); ¹³C NMR (100 MHz, DMSO-*d*₆) δ 162.4, 162.0, 150.1, 149.0, 147.9, 133.1, 129.9, 125.2, 121.6, 114.7, 111.3, 108.0, 70.2, 59.9. HRMS (ESI) *m/z* 333.1073 [M + H]⁺ (calcd for C₁₆H₁₇N₂O₆, 333.1087).

2.1.5. (*E*)-4-(methylsulfonyl)-*N'*-(2,3,4-trihydroxybenzylidene)benzohydrazide (**3c**)

Yield 79.6%. ¹H NMR (400 MHz, DMSO-*d*₆) δ 12.20 (s, 1H), 11.36 (s, 1H), 9.59 (s, 1H), 8.56 (s, 1H), 8.50 (s, 1H), 8.16 (d, *J* = 8.5 Hz, 2H), 8.10 (d, *J* = 8.5 Hz, 2H), 6.84 (d, *J* = 8.5 Hz, 1H), 6.42 (d, *J* = 8.4 Hz, 1H), 3.30 (s, 3H); ¹³C NMR (100 MHz, DMSO-*d*₆) δ 161.7, 151.3, 149.4, 148.0, 143.8, 137.9, 133.1, 129.0, 127.6, 121.7, 111.2, 108.2, 43.7. HRMS (ESI) *m/z* 351.0652 [M + H]⁺ (calcd for C₁₅H₁₅N₂O₆S, 351.0651).

2.1.6. (*E*)-3-(methylsulfonyl)-*N'*-(2,3,4-trihydroxybenzylidene)benzohydrazide (**3d**)

Yield 85.5%. ¹H NMR (400 MHz, DMSO-*d*₆) δ 12.23 (s, 1H), 11.38 (s, 1H), 9.57 (s, 1H), 8.56 (brs, 1H), 8.51 (s, 1H), 8.46 (t, *J* = 1.5 Hz, 1H), 8.27 (d, *J* = 7.9 Hz, 1H), 8.16 (d, *J* = 9.4 Hz, 1H), 7.84 (t, *J* = 7.8 Hz, 1H), 6.84 (d, *J* = 8.5 Hz, 1H), 6.42 (d, *J* = 8.5 Hz, 1H), 3.30 (s, 3H); ¹³C NMR (100 MHz, DMSO-*d*₆) δ 161.4, 151.2, 149.4, 148.0, 141.6, 134.4, 133.2, 133.0, 130.5, 130.4, 126.4, 121.6, 111.2, 108.2, 43.9. HRMS (ESI) *m/z* 351.0639 [M + H]⁺ (calcd for C₁₅H₁₅N₂O₆S, 351.0651).

2.1.7. (*E*)-4-butyl-*N'*-(2,3,4-trihydroxybenzylidene)benzohydrazide (**3e**)

Yield 64.3%. ¹H NMR (400 MHz, DMSO-*d*₆) δ 11.91 (s, 1H), 11.57 (s, 1H), 9.50 (s, 1H), 8.51 (brs, 1H), 8.45 (s, 1H), 7.85 (d, *J* = 8.2 Hz, 2H), 7.36 (d, *J* = 8.2 Hz, 2H), 6.78 (d, *J* = 8.5 Hz, 1H), 6.40 (d, *J* = 8.4 Hz, 1H), 2.68 (t, *J* = 7.6 Hz, 2H), 1.62–1.55 (m, 2H), 1.36–1.27 (m, 2H), 0.91 (t, *J* = 7.3 Hz, 3H); ¹³C NMR (100 MHz, DMSO-*d*₆) δ 162.9, 150.4, 149.1, 147.9, 147.1, 133.1, 130.7, 128.9, 128.0, 121.6, 111.3, 108.0, 35.1, 33.3, 22.1, 14.2. HRMS (ESI) *m/z* 329.1485 [M + H]⁺ (calcd for C₁₈H₂₁N₂O₄, 329.1501).

2.1.8. (*E*)-3-chloro-*N'*-(2,3,4-trihydroxybenzylidene)benzohydrazide (**3f**)

Yield 88.9%. ¹H NMR (400 MHz, DMSO-*d*₆) δ 12.06 (s, 1H), 11.40 (s, 1H), 9.56 (s, 1H), 8.55 (s, 1H), 8.47 (s, 1H), 7.97 (t, *J* = 1.8 Hz, 1H), 7.90–7.88 (m, 1H), 7.70–7.67 (m, 1H), 7.58 (t, *J* = 7.9 Hz, 1H), 6.82 (d, *J* = 8.5 Hz, 1H), 6.41 (d, *J* = 8.4 Hz, 1H); ¹³C NMR (100 MHz, DMSO-*d*₆) δ 161.5, 151.0, 149.3, 148.0, 135.3, 133.8, 133.1, 132.1, 131.0, 127.7, 126.8, 121.6, 111.2, 108.1. HRMS (ESI) *m/z* 307.0494 [M + H]⁺ (calcd for C₁₄H₁₂ClN₂O₄, 307.0486).

2.1.9. (*E*)-4-chloro-*N'*-(2,3,4-trihydroxybenzylidene)benzohydrazide (**3g**)

Yield 65.3%. ¹H NMR (400 MHz, DMSO-*d*₆) δ 12.04 (s, 1H), 11.46 (s, 1H), 9.55 (s, 1H), 8.54 (s, 1H), 8.47 (s, 1H), 7.96–7.94 (m, 2H), 7.62 (d, *J* = 8.6 Hz, 2H), 6.81 (d, *J* = 8.5 Hz, 1H), 6.41 (d, *J* = 8.4 Hz, 1H); ¹³C NMR (100 MHz, DMSO-*d*₆) δ 161.9, 150.8, 149.3, 148.0, 137.1, 133.1, 132.1, 129.9, 129.1, 121.6, 111.2, 108.1. HRMS (ESI) *m/z* 307.0494 [M + H]⁺ (calcd for C₁₄H₁₂ClN₂O₄, 307.0486).

2.1.10. (*E*)-4-methyl-*N'*-(2,3,4-trihydroxybenzylidene)benzenesulfonohydrazide (**3h**)

Yield 76.6%. ¹H NMR (400 MHz, DMSO-*d*₆) δ 11.28 (s, 1H), 10.06 (s, 1H), 9.57 (s, 1H), 8.50 (s, 1H), 8.02 (s, 1H), 7.73 (d, *J* = 8.3 Hz, 2H), 7.43 (d, *J* = 8.1 Hz, 2H), 6.73 (d, *J* = 8.6 Hz, 1H), 6.34 (d, *J* = 8.5 Hz, 1H), 2.37 (s, 3H); ¹³C NMR (100 MHz, DMSO-*d*₆) δ 150.3, 149.2, 147.2, 144.1, 136.1, 133.0, 130.2, 127.6, 120.4, 111.3, 108.1, 21.4. HRMS (ESI) *m/z* 323.0699 [M + H]⁺ (calcd for C₁₄H₁₅N₂O₅S, 323.0702).

2.1.11. (*E*)-4-methoxy-*N'*-(2,3,4-trihydroxybenzylidene)benzohydrazide (**3i**)

Yield 74.9%. ¹H NMR (400 MHz, DMSO-*d*₆) δ 11.86 (s, 1H), 11.62 (s, 1H), 9.49 (s, 1H), 8.52 (s, 1H), 8.45 (s, 1H), 7.92 (d, *J* = 8.8 Hz, 2H), 7.08 (d, *J* = 8.9 Hz, 2H), 6.77 (d, *J* = 8.5 Hz, 1H), 6.40 (d, *J* = 8.4 Hz, 1H), 3.84 (s, 3H); ¹³C NMR (100 MHz, DMSO-*d*₆) δ 162.5, 162.4, 150.1, 149.0, 147.9, 133.1, 129.9, 125.3, 121.6, 114.2, 111.3, 108.0, 55.9. HRMS (ESI) *m/z* 303.0984 [M + H]⁺ (calcd for C₁₅H₁₅N₂O₅, 303.0981).

2.1.12. (*E*)-4-nitro-*N'*-(2,3,4-trihydroxybenzylidene)benzohydrazide (**3j**)

Yield 85.0%. ¹H NMR (400 MHz, DMSO-*d*₆) δ 12.26 (s, 1H), 11.33 (s, 1H), 9.60 (s, 1H), 8.56 (brs, 1H), 8.50 (s, 1H), 8.38 (d, *J* = 12.0 Hz, 2H), 8.16 (d, *J* = 12.0 Hz, 2H), 6.84 (d, *J* = 8.5 Hz, 1H), 6.42 (d, *J* = 8.5 Hz, 1H); ¹³C NMR (100 MHz, DMSO-*d*₆) δ 161.3, 151.5, 149.7, 149.5, 148.0, 139.0, 133.1, 129.5, 124.1, 121.7, 111.2, 108.2. HRMS (ESI) *m/z* 318.0723 [M + H]⁺ (calcd for C₁₄H₁₂N₃O₆, 318.0726).

2.1.13. (*E*)-3-methoxy-*N'*-(2,3,4-trihydroxybenzylidene)benzohydrazide (**3k**)

Yield 81.8%. ¹H NMR (400 MHz, DMSO-*d*₆) δ 11.94 (s, 1H), 11.52 (s, 1H), 9.53 (s, 1H), 8.54 (brs, 1H), 8.47 (s, 1H), 7.52–7.44 (m, 3H), 7.19–7.16 (m, 1H), 6.79 (d, *J* = 8.5 Hz, 1H), 6.41 (d, *J* = 8.4 Hz, 1H), 3.84 (s, 3H); ¹³C NMR (100 MHz, DMSO-*d*₆) δ 162.7, 159.7, 150.7, 149.2, 147.9, 134.7, 133.1, 130.2, 121.6, 120.2, 118.0, 113.2, 111.2, 108.1, 55.8. HRMS (ESI) *m/z* 303.0972 [M + H]⁺ (calcd for C₁₅H₁₅N₂O₅, 303.0981).

2.1.14. (*E*)-2-phenyl-*N'*-(2,3,4-trihydroxybenzylidene)acetohydrazide (**3l**)

Yield 66.3%. ¹H NMR (400 MHz, DMSO-*d*₆) δ 11.72 (s, 1H), 11.30 (s, 1H), 9.49 (s, 1H), 8.49 (s, 1H), 8.23 (s, 1H), 7.35–7.27 (m, 5H), 6.77 (d, *J* = 8.5 Hz, 1H), 6.38 (d, *J* = 8.5 Hz, 1H), 3.54 (s, 2H); ¹³C NMR (100 MHz, DMSO-*d*₆) δ 166.4, 149.4, 149.1, 147.8, 136.0, 133.1, 129.5, 128.8, 127.1, 121.5, 111.1, 108.0, 41.3. HRMS (ESI) *m/z* 287.1036 [M + H]⁺ (calcd for C₁₅H₁₅N₂O₄, 287.1032).

2.1.15. (*E*)-3-nitro-*N'*-(2,3,4-trihydroxybenzylidene)benzohydrazide (**3m**)

Yield 69.2%. ¹H NMR (400 MHz, DMSO-*d*₆) δ 12.29 (s, 1H), 11.34 (s, 1H), 9.59 (s, 1H), 8.78 (t, *J* = 1.9 Hz, 1H), 8.56 (brs, 1H), 8.52 (s, 1H), 8.47–8.37 (m, 2H), 7.86 (t, *J* = 8.0 Hz, 1H), 6.85 (d, *J* = 8.5 Hz, 1H), 6.42 (d, *J* = 8.4 Hz, 1H); ¹³C NMR (100 MHz, DMSO-*d*₆) δ 160.8, 151.3, 149.4, 148.2, 148.0, 134.8, 134.5, 133.2, 130.8, 126.8, 122.6, 121.6, 111.2, 108.2. HRMS (ESI) *m/z* 318.0721 [M + H]⁺ (calcd for C₁₄H₁₂N₃O₆, 318.0726).

2.1.16. (*E*)-*N'*-(2,3,4-trihydroxybenzylidene)-[1,1'-biphenyl]-4-carbohydrazide (**3n**)

Yield 70.5%. ¹H NMR (400 MHz, DMSO-*d*₆) δ 12.06 (s, 1H), 11.57 (s, 1H), 9.56 (s, 1H), 8.57 (s, 1H), 8.50 (s, 1H), 8.04 (d, *J* = 8.3 Hz, 2H), 7.85 (d, *J* = 8.3 Hz, 2H), 7.76 (d, *J* = 7.4 Hz, 2H), 7.53–7.41 (m, 3H), 6.81 (d, *J* = 8.5 Hz, 1H), 6.42 (d, *J* = 8.4 Hz, 1H); ¹³C NMR (100 MHz, DMSO-*d*₆) δ 162.6, 150.6, 149.2, 147.9, 143.8, 139.4, 133.1, 132.0, 129.5, 128.7, 127.4, 127.2, 121.6, 111.3, 108.1. HRMS (ESI) *m/z* 349.1238 [M + H]⁺ (calcd for C₂₀H₁₇N₂O₄, 349.1188).

2.1.17. (*E*)-*N'*-(2,3,4-trihydroxybenzylidene)-2,3-dihydrobenzo[*b*][1,4]dioxine-2-carbohydrazide (**3o**)

Yield 82.2%. ¹H NMR (400 MHz, DMSO-*d*₆) δ 11.74 (s, 1H), 11.18 (s, 1H), 9.56 (s, 1H), 8.54 (s, 1H), 8.41 (s, 1H), 7.05–7.02 (m, 1H), 6.92–6.85 (m, 3H), 6.77 (d, *J* = 8.5 Hz, 1H), 6.39 (d, *J* = 8.5 Hz, 1H), 5.00–4.99 (m, 1H), 4.43–4.33 (m, 2H); ¹³C NMR (100 MHz, DMSO-*d*₆) δ 163.4, 151.5, 149.4, 147.9, 143.4, 142.5, 133.1, 122.2, 122.1, 121.6, 117.8, 117.6, 111.0, 108.2, 72.5, 65.0. HRMS (ESI) *m/z* 331.0913 [M + H]⁺ (calcd for C₁₆H₁₅N₂O₆, 331.0930).

2.1.18. (*E*)-6-hydroxy-*N'*-(2,3,4-trihydroxybenzylidene)-2-naphthohydrazide (**3p**)

Yield 63.8%. ¹H NMR (400 MHz, DMSO-*d*₆) δ 12.04 (s, 1H), 11.64 (s, 1H), 10.16 (s, 1H), 9.51 (s, 1H), 8.54 (brs, 1H), 8.50 (s, 1H), 8.43 (s, 1H), 7.95–7.89 (m, 2H), 7.81 (d, *J* = 8.7 Hz, 1H), 7.21 (s, 1H), 7.19 (d, *J* = 8.7 Hz, 2H), 6.80 (d, *J* = 8.5 Hz, 1H), 6.42 (d, *J* = 8.4 Hz, 1H); ¹³C NMR (100 MHz, DMSO-*d*₆) δ 163.1, 157.6, 150.2, 149.1, 147.9, 136.8, 133.1, 131.2, 128.5, 127.3, 127.0, 126.7, 124.8, 121.6, 120.0, 111.3, 109.1, 108.1. HRMS (ESI) *m/z* 339.0973 [M + H]⁺ (calcd for C₁₈H₁₅N₂O₅, 339.0981).

2.1.19. (*E*)-*N'*-(4-[2-(2,3,4-trihydroxybenzylidene)hydrazine-1-carbonyl]phenyl)cyclopropanecarboxamide (**3q**)

Yield 76.9%. ¹H NMR (400 MHz, DMSO-*d*₆) δ 11.88 (s, 1H), 11.59 (s, 1H), 10.52 (s, 1H), 9.50 (s, 1H), 8.51 (s, 1H), 8.44 (s, 1H), 7.89 (d, *J* = 8.7 Hz, 2H), 7.73 (d, *J* = 8.8 Hz, 2H), 6.78 (d, *J* = 8.5 Hz, 1H), 6.40 (d, *J* = 8.4 Hz, 1H), 1.85–1.79 (m, 1H), 0.85–0.83 (m, 4H); ¹³C NMR (100 MHz, DMSO-*d*₆) δ 172.6, 162.4, 150.2, 149.1, 147.9, 142.9, 133.1, 129.0, 127.3, 121.6, 118.7, 111.3, 108.0, 15.1, 8.0. HRMS (ESI) *m/z* 356.1240 [M + H]⁺ (calcd for C₁₈H₁₈N₃O₅, 356.1246).

2.1.20. (*E*)-5-hydroxy-*N'*-(2,3,4-trihydroxybenzylidene)-3H-indole-2-carbohydrazide (**3r**)

Yield 73.0%. ¹H NMR (400 MHz, DMSO-*d*₆) δ 11.93 (s, 1H), 11.54 (s, 1H), 11.49 (s, 1H), 9.51 (s, 1H), 8.91 (s, 1H), 8.52 (s, 1H), 8.45 (s, 1H), 7.28 (d, *J* = 8.8 Hz, 1H), 7.07–7.10 (m, 1H), 6.93 (d, *J* = 2.2 Hz, 1H), 6.82–6.77 (m, 2H), 6.41 (d, *J* = 8.4 Hz, 1H); ¹³C NMR (100 MHz, DMSO-*d*₆) δ 157.6, 151.7, 149.6, 149.1, 147.8, 133.1, 132.1, 130.3, 128.1, 121.4, 115.6, 113.3, 111.4, 108.1, 104.8, 103.1. HRMS (ESI) *m/z* 328.0928 [M + H]⁺ (calcd for C₁₆H₁₄N₃O₅, 328.0933).

2.1.21. (*E*)-*N'*-(2,3,4-trihydroxybenzylidene)nicotinohydrazide (**3s**)

Yield 87.2%. ¹H NMR (400 MHz, DMSO-*d*₆) δ 12.20 (s, 1H), 11.44 (s, 1H), 9.60 (s, 1H), 9.16 (m, 1H), 8.86 (dd, *J* = 4.9, 1.7 Hz, 1H), 8.60 (s, 1H), 8.55 (s, 1H), 8.35 (dt, *J* = 8.0, 2.0 Hz, 1H), 7.65–7.68 (m, 1H), 6.91 (d, *J* = 8.5 Hz, 1H), 6.49 (d, *J* = 8.4 Hz, 1H); ¹³C NMR (100 MHz, DMSO-*d*₆) δ 161.5, 152.8, 151.0, 149.4, 149.0, 148.0, 135.8, 133.1, 129.2, 124.1, 121.6, 111.2, 108.2. HRMS (ESI) *m/z* 274.0811 [M + H]⁺ (calcd for C₁₃H₁₂N₃O₄, 274.0828).

2.1.22. (*E*)-2-hydroxy-*N'*-(2,3,4-trihydroxybenzylidene)benzohydrazide (**3t**)

Yield 81.0%. ¹H NMR (400 MHz, DMSO-*d*₆) δ 11.93 (s, 1H), 11.86 (s, 1H), 11.38 (s, 1H), 9.53 (s, 1H), 8.52 (d, *J* = 1.6 Hz, 2H), 7.89 (dd, *J* = 7.9, 1.7 Hz, 1H), 7.43–7.47 (m, 1H), 7.02–6.92 (m, 2H), 6.82 (d, *J* = 8.5 Hz, 1H), 6.41 (d, *J* = 8.4 Hz, 1H); ¹³C NMR (100 MHz, DMSO-*d*₆) δ 164.6, 159.5, 151.3, 149.4, 148.0, 134.3, 133.1, 128.8, 121.6, 119.4, 117.7, 115.9, 111.2, 108.2. HRMS (ESI) *m/z* 289.0776 [M + H]⁺ (calcd for C₁₄H₁₃N₂O₅, 289.0824).

2.1.23. (*E*)-4-fluoro-*N'*-(2,3,4-trihydroxybenzylidene)benzohydrazide (**3u**)

Yield 62.5%. ¹H NMR (400 MHz, DMSO-*d*₆) δ 11.96 (s, 1H), 11.48 (s, 1H), 9.46 (s, 1H), 8.47 (s, 1H), 8.05–7.96 (m, 2H), 7.38 (t, *J* = 8.8 Hz, 2H), 6.80 (d, *J* = 8.4 Hz, 1H), 6.41 (d, *J* = 8.4 Hz, 1H); ¹³C NMR (100 MHz, DMSO-*d*₆) δ 163.4, 161.9, 150.6, 149.2, 147.9, 133.1, 130.7, 130.6, 129.8, 129.8, 121.6, 116.1, 115.8, 111.2, 108.1. HRMS (ESI) *m/z* 291.0739 [M + H]⁺ (calcd for C₁₄H₁₂FN₂O₄, 291.0781).

2.1.24. (*E*)-4-chloro-3-nitro-*N'*-(2,3,4-trihydroxybenzylidene)benzohydrazide (**3v**)

Yield 73.6%. ¹H NMR (400 MHz, DMSO-*d*₆) δ 12.21 (s, 1H), 11.24 (s, 1H), 9.53 (s, 1H), 8.60 (d, *J* = 2.1 Hz, 1H), 8.50 (d, *J* = 7.9 Hz, 2H), 8.23 (dd, *J* = 8.4, 2.2 Hz, 1H), 7.99 (d, *J* = 8.4 Hz, 1H), 6.85 (d, *J* = 8.5 Hz, 1H), 6.42 (d, *J* = 8.5 Hz, 1H); ¹³C NMR (100 MHz, DMSO-*d*₆) δ 160.0, 151.3, 149.5, 148.0, 147.8, 133.5, 133.1, 133.1, 132.6, 128.8, 125.2, 121.5, 111.2, 108.2. HRMS (ESI) *m/z* 352.0306 [M + H]⁺ (calcd for C₁₄H₁₁ClN₃O₆, 352.0336).

2.1.25. (*E*)-*N'*-(2,3,4-trihydroxybenzylidene)thiophene-2-carbohydrazide (**3w**)

Yield 60.4%. ¹H NMR (400 MHz, DMSO-*d*₆) δ 11.99 (s, 1H), 11.34 (s, 1H), 9.49 (s, 1H), 8.52 (s, 1H), 8.44 (s, 2H), 7.89 (dd, *J* = 4.3, 2.8 Hz, 2H), 7.26–7.22 (m, 1H), 6.81 (d, *J* = 8.5 Hz, 1H), 6.40 (d, *J* = 8.4 Hz, 1H); ¹³C NMR (100 MHz, DMSO-*d*₆) δ 157.6, 150.2, 149.2, 147.8, 138.2, 133.1, 132.3, 129.3, 128.6, 121.4, 111.3, 108.1. HRMS (ESI) *m/z* 279.0465 [M + H]⁺ (calcd for C₁₂H₁₁N₂O₄S, 279.0440).

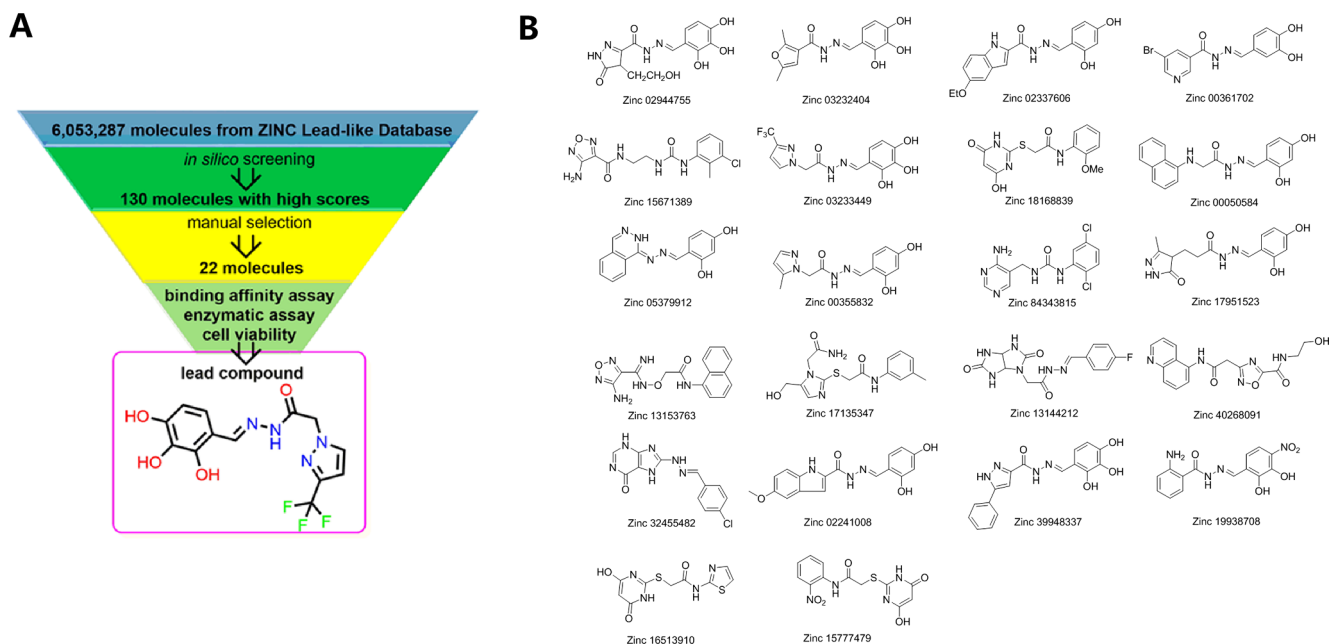


Fig. 1. Discovery of leads as HK2 inhibitor. (A) Procedure for screening active lead compounds. (B) Chemical structure of 22 compounds by virtual screening from ZINC database.

Table 1

Predicted binding free energies and inhibitory activities of screening hits.

ZINC number	ICM scores ^a	IC ₅₀ for enzyme activities (μM)	K _d values ^b (μM)	Cell IC ₅₀ (μM) ^d
02944755	-38.28	> 50	69.80 ± 5.90	> 200
03232404	-37.82	8.17 ± 0.12	69.30 ± 3.20	102.30 ± 11.20
02337606	-37.14	> 50	431.20 ± 65.20	> 200
00361702	-37.02	> 50	6920.00 ± 99.80	> 200
15671389	-34.49	> 50	286.20 ± 34.80	> 200
03233449	-33.77	9.39 ± 0.11	41.70 ± 3.60	87.30 ± 6.90
18168839	-40.66	> 50	242.00 ± 38.60	> 200
00050584	-32.99	> 50	n.b. ^c	> 200
05379912	-34.30	> 50	206.20 ± 17.30	> 200
00355832	-33.87	> 50	n.b.	> 200
84343815	-32.29	> 50	n.b.	> 200
17951523	-32.20	> 50	n.b.	> 200
13153763	-32.05	> 50	n.b.	> 200
17135347	-34.72	> 50	313.20 ± 16.20	> 200
13144212	-32.47	> 50	n.b.	> 200
40268091	-32.39	> 50	1530.00 ± 194.00	> 200
32455482	-32.84	> 50	n.b.	> 200
02241008	-38.14	> 50	n.b.	> 200
39948337	-32.64	10.10 ± 0.21	233.00 ± 35.10	94.70 ± 7.20
19938708	-35.38	> 50	n.b.	> 200
16513910	-44.62	> 50	296.00 ± 6.50	> 200
15777479	-35.91	> 50	n.b.	> 200

^a Docking score/interaction potential of compounds with HK2 (kcal/mol).

^b The K_d value is automatic calculated by the curve fitting, and presents as means ± SD for three experiments.

^c n.b is no clear binding detected in the MST measurement.

^d SW480 cell was used to determine IC₅₀.

2.1.26. (*E*)-*N'*-(2,3,4-trihydroxybenzylidene)isonicotinohydrazide (**3x**)

Yield 54.8%. ¹H NMR (400 MHz, DMSO-*d*₆) δ 12.18 (s, 1H), 12.19 (s, 1H), 9.56 (s, 1H), 8.79–8.81 (m, 2H), 8.55 (s, 1H), 8.50 (s, 1H), 7.83–7.85 (m, 2H), 6.84 (d, *J* = 8.5 Hz, 1H), 6.42 (d, *J* = 8.5 Hz, 1H); ¹³C NMR (100 MHz, DMSO-*d*₆) δ 161.4, 151.5, 150.8, 149.5, 148.0, 140.5, 133.1, 133.1, 121.9, 121.6, 111.2, 108.2. HRMS (ESI) *m/z* 274.0822 [M + H]⁺ (calcd for C₁₃H₁₂N₃O₄, 274.0828).

2.1.27. (*E*)-2,5-dihydroxy-*N'*-(2,3,4-trihydroxybenzylidene)benzohydrazide (**3y**)

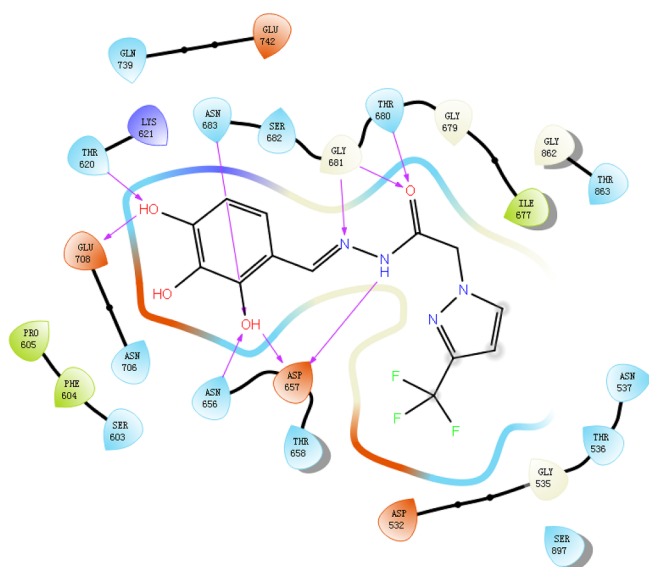
Yield 68.8%. ¹H NMR (400 MHz, DMSO-*d*₆) δ 11.84 (s, 1H), 11.44 (s, 1H), 11.10 (s, 1H), 9.51 (s, 1H), 9.13 (s, 1H), 8.49 (s, 1H), 7.28 (d,

J = 3.0 Hz, 1H), 6.90 (dd, *J* = 8.8, 3.0 Hz, 1H), 6.85–6.76 (m, 2H), 6.40 (d, *J* = 8.5 Hz, 1H); ¹³C NMR (100 MHz, DMSO-*d*₆) δ 164.2, 151.8, 151.2, 150.0, 149.3, 148.0, 133.1, 121.9, 121.7, 118.3, 116.1, 114.2, 111.2, 108.1. HRMS (ESI) *m/z* 305.0779 [M + H]⁺ (calcd for C₁₄H₁₃N₂O₆, 305.0774).

2.1.28. (*E*)-*N'*-(2,3,4-trihydroxybenzylidene)benzohydrazide (**3z**)

Yield 76.6%. ¹H NMR (400 MHz, DMSO-*d*₆) δ 11.94 (s, 1H), 11.52 (s, 1H), 9.46 (s, 1H), 8.49 (s, 1H), 8.44 (s, 1H), 7.91–7.88 (m, 2H), 7.59–7.55 (m, 1H), 7.53–7.49 (m, 2H), 6.76 (d, *J* = 8.5 Hz, 1H), 6.37 (d, *J* = 8.5 Hz, 1H); ¹³C NMR (100 MHz, DMSO-*d*₆) δ 162.9, 150.5, 149.1, 147.9, 133.3, 133.1, 132.2, 128.9, 127.9, 121.6, 111.2, 108.0.

A



B

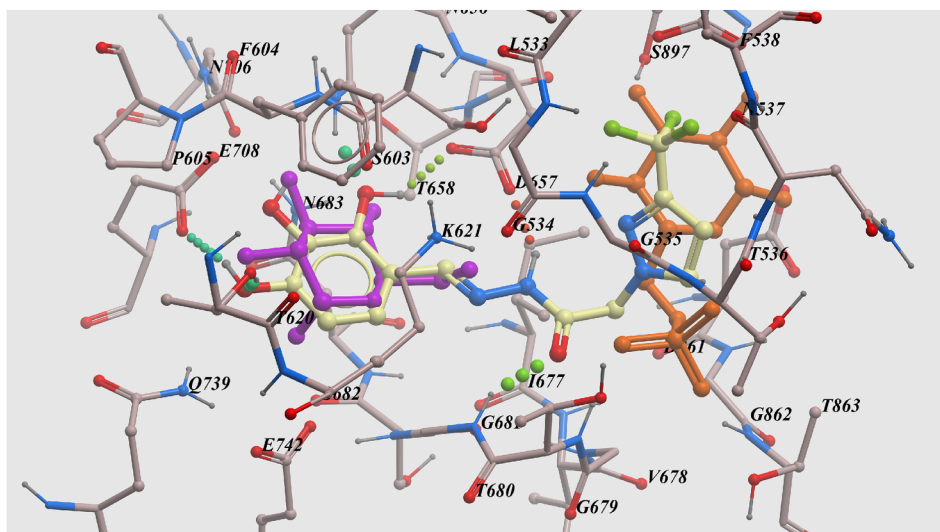


Fig. 2. The analysis of the lead compound binding mode in the HK2 pocket. (A) Ligand interaction diagram of the lead compound zinc 03233449 with HK2 (PDB code: 2NZT) (B) Low-energy binding conformations of zinc03233449 bound to HK2 generated by virtual ligand docking. Zinc03233449 formed a series of H-bond interactions with HK2 residues. Zinc03233449 (yellow), substrate glucose (purple) and product glucose-6-phosphate (brown) were depicted as ball-and-stick model. The trihydroxybenzene ring fragment of zinc03233449 occupied the binding site of the substrate glucose and they are almost completely overlapped. The trifluoromethylpyrazole part of zinc03233449 is inserted into the binding pocket of product glucose-6-phosphate.

HRMS (ESI) m/z 273.0877 $[M + H]^+$ (calcd for $C_{14}H_{13}N_2O_4$, 273.0875).

2.2. Biology

2.2.1. Clone, expression and purification of HK2

Human HK2 aa17-916 with an N-terminal His tag and thrombin cleavage site was cloned into pET28-LIC. All proteins were expressed in *E. coli* BL21 (DE3) Codon Plus (Invitrogen). Cultures were grown in LB media containing 50 mg/L kanamycin and 50 mg/L chloramphenicol at 37 °C to OD 0.6–0.8, then induced at 20 °C with 0.5 mM IPTG for 20 h. Cultures were harvested by centrifugation at 4000 g for 10 min. HK2 was purified with Ni-agarose affinity chromatography, followed by anion exchange chromatography and size exclusion chromatography. The purified proteins were stored in 25 mM phosphate pH 8 containing 50 mM Tris pH 8 containing 150 mM NaCl.

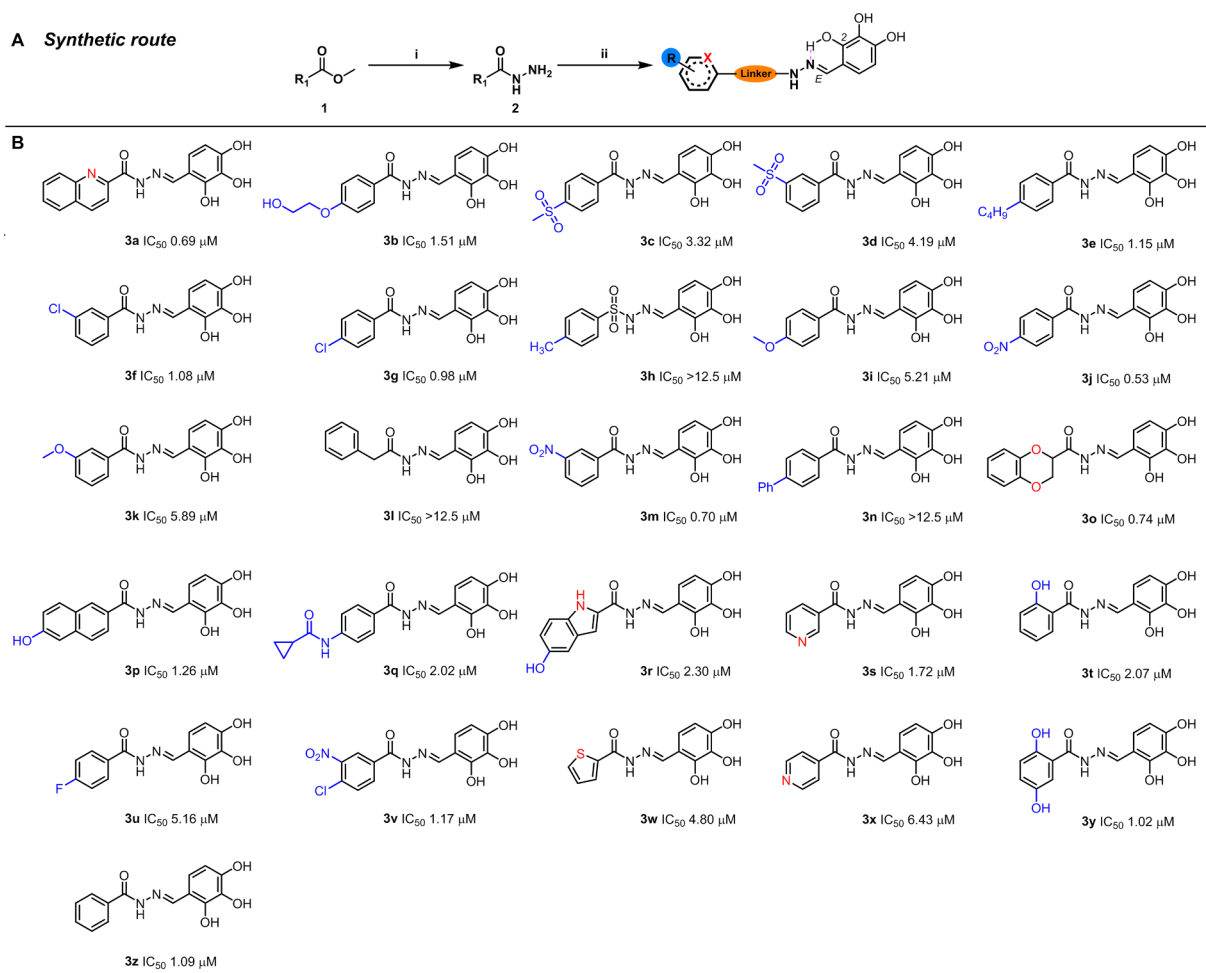
2.2.2. In vitro enzyme inhibition assay

Specific details were referred to our previous work and with a little modification. To assay the inhibitory effects of compounds on HK2, NADH which was generated through a coupled reaction with glucose-6-phosphate dehydrogenase (G6P-DH) was monitored by optical density

at 340 nm every minute for 15 min on a SpectraMax M5e plate read. Briefly, 30 μ L recombinant HK2 (0.3 μ M) was incubated with 10 μ L compounds at 37 °C for 10 min. Then 70 μ L assay mix containing 100 mM Tris-HCl pH 8.0, 200 mM Glucose, 5 mM $MgCl_2$, 1 mM NAD^+ , 0.8 mM ATP, 0.25 Units of G6P-DH, was added. The enzyme inhibition IC_{50} values for compounds were calculated based on the changes in absorbance. No Compounds interference with G6P-DH activity was observed.

2.2.3. Microscale thermophoresis (MST) assay

Specific details were referred to our previous work and with a little modification. Briefly, Labelled HK2 was kept constant at 20 nM, and all tested samples were 1:1 diluted in a 20 mM HEPES (pH 7.4), 1% (v/v) DMSO and 0.05 (v/v) % Tween-20. After 10 min incubation at room temperature, samples were loaded into Monolith™ standard-treated capillaries. And the thermophoresis was measured at room temperature after 30 min incubation on a Monolith NT.115 instrument (Germany). Furthermore, laser power was set to 40% using 30 sec on-time. The LED power was set to 50%. The dissociation constant K_d values were fitted by using the NT-Analysis software.



Scheme 1. Rational design and synthetic strategy for the HK2 inhibitors. (A) Reagents and conditions: (i) 40% Hydrazine hydrate (5.0 equiv.), in MeOH, reflux. (ii) 2,3,4-Trihydroxybenzaldehyde (1.1 equiv), in MeOH, rt. (B) Synthesized compounds **3a-3z** and their enzymatic inhibition IC₅₀.

2.2.4. Molecular docking

Crystal structures of human HK2 (PDB code: 2N2T) was obtained from the Protein Data Bank. The docking was operated by using ICM 3.8.2 modeling software on an Intel i7 4960 processor (MolSoft LLC, San Diego, CA). Ligand binding pocket residues were selected by using graphical tools in the ICM software, to create the boundaries of the docking search. In the docking calculation, potential energy maps of the receptor were calculated using default parameters. Compounds were inputted into ICM and an index file was created. Conformational sampling was based on the Monte Carlo procedure³⁰, and finally the lowest-energy and the most favorable orientation of the ligand were selected.

2.2.5. Cell culture

Human colon cancer cells SW480 and human pancreatic cancer cells SW1990 were obtained from the American Type Culture Collection (ATCC, USA) and grown in high Glucose Dulbecco's modified Eagle's medium supplemented with 2 mM glutamine, 10% (v/v) fetal bovine serum (FBS), 100 U/mL penicillin and 100 mg/mL streptomycin. Cell cultures were grown and maintained in culture at 37 °C in a humidified tissue culture incubator with 5% CO₂ using standard tissue procedures. Cell lines, HCT116(CCL-247), SW620(CCL-227), PANC-1(CRL-1469), Aspc-1(CRL-1682) were purchased from ATCC.

2.2.6. Cytotoxicity test

SW480 or SW1990 cells were incubated with tested compounds for 48 h and its cytotoxicity was measured using a Cell Counting Kit-8

(CCK-8).

2.2.7. Western blot analysis

Lysate protein (20–40 μg) was subjected to 10% SDS-PAGE and electrophoretically transferred to polyvinylidene difluoride membranes (PVDF) (Millipore, USA). The membranes were sequentially blocked with 5% non-fat milk, and incubated overnight with the following primary antibodies: β-actin (A2228) (1:1000), HK2 (#2867) (1:1000). Protein bands were visualized using an enhanced chemiluminescence reagent (ECL Plus) (GE Healthcare, USA) after hybridization with a HRP conjugated secondary antibody.

2.3. Statistical analysis

All values are expressed as the mean ± SD. Comparisons between multiple-group means were performed using one-way analysis of variance (one-way ANOVA). P values < 0.05 were statistically significant. All statistical analyses were performed using GraphPad Prism software version 5.0.

3. Results and discussion

3.1. Screening, rational design of HK2 inhibitors

Structure-based virtual ligand screening was performed using the ICM-Pro 3.8.2 modeling software (MolSoft LLC, San Diego, CA) [22]. From 6,053,287 molecules, 130 screen hits with significant ICM scores

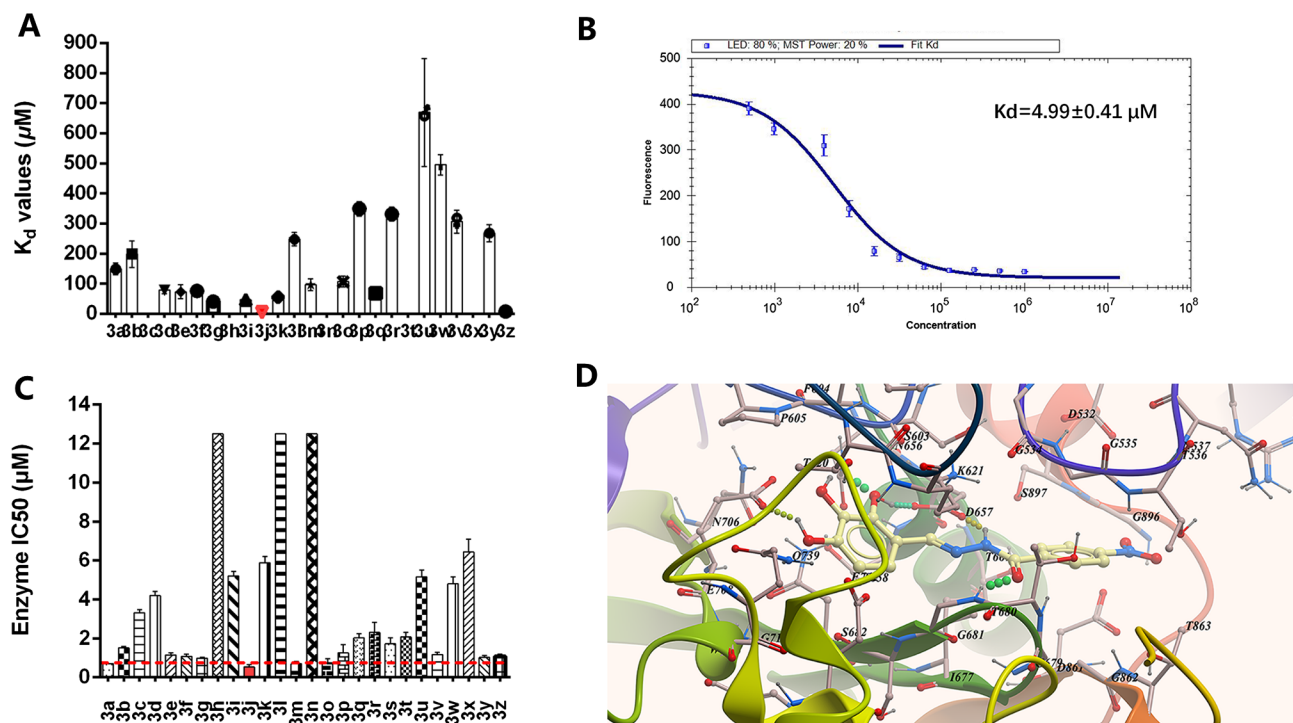


Fig. 3. Compound 3j binds to HK2 and inhibits HK2 enzyme activity *in vitro*. (A) The equilibrium dissociation constants (K_d) of compounds (3a–3z). (B) MST assay identifying the binding of compound 3j to HK2. (C) The enzymatic activity inhibition assay of compounds (3a–3z). (D) The binding pockets analysis of compound 3j on HK2 (docking model from PDB code 2NZT).

Table 2

The equilibrium dissociation constants (K_d) and inhibitory activity on HK2 enzyme activity *in vitro*.

Compounds	K_d values ^a (μM)	Enzyme IC_{50} (μM)
3a	149.00 \pm 19.30	0.69 \pm 0.02
3b	198.00 \pm 43.80	1.51 \pm 0.08
3c	n.b. ^b	3.32 \pm 0.15
3d	78.40 \pm 11.40	4.19 \pm 0.23
3e	73.30 \pm 22.90	1.15 \pm 0.12
3f	75.90 \pm 11.90	1.08 \pm 0.11
3g	40.60 \pm 7.42	0.98 \pm 0.05
3h	n.b.	> 12.5
3i	47.10 \pm 5.80	5.21 \pm 0.23
3j	4.99 \pm 0.41	0.53 \pm 0.13
3k	55.40 \pm 14.60	5.89 \pm 0.31
3l	248.00 \pm 22.50	> 12.50
3m	96.60 \pm 19.60	0.70 \pm 0.12
3n	n.b.	> 12.5
3o	107.00 \pm 18.50	0.74 \pm 0.21
3p	349.00 \pm 23.80	1.26 \pm 0.41
3q	67.50 \pm 9.32	2.02 \pm 0.23
3r	331.00 \pm 23.10	2.30 \pm 0.52
3s	562.00 \pm 83.10	1.72 \pm 0.32
3t	n.b.	2.07 \pm 0.25
3u	669.00 \pm 179.00	5.16 \pm 0.34
3v	306.00 \pm 38.60	1.17 \pm 0.11
3w	495.00 \pm 33.90	4.80 \pm 0.35
3x	n.b.	6.43 \pm 0.67
3y	268.00 \pm 28.40	1.02 \pm 0.09
3z	7.63 \pm 0.77	1.08 \pm 0.04
Metformin	31400.00 \pm 1300.00	> 10,000
2-Deoxyglucose	n.b.	> 10,000
3-Bromopyruvate	26.10 \pm 3.13	0.60 \pm 0.05

^a The K_d value is automatically calculated by the curve fitting and presents as means \pm SD for three experiments.

^b n.b. is no clear binding detected in the MST measurement.

and high occupancy of the active binding pocket were obtained. After further screening to eliminate highly similar structures, 22 hits (MolPort, Latvia) were manually selected for further evaluation (Fig. 1A and B, Table 1). Three lead compounds with ZINC codes of 03232404, 03233449, and 39948337, sharing the same fragment as (*E*)-*N'*-(2,3,4-trihydroxybenzylidene) arylhydrazide, exhibited significant enzyme inhibitory effects. A simple structure–activity relationship (SAR) analysis showed that the trihydroxybenzene ring was essential for enzyme inhibitory activity.

Further modifications were made to these compounds based on the analysis of their binding mode in the HK2 pocket (Fig. 2A). From a generated docking model, the compound adopted an extended conformation, in which the pyrogallol part of the compound was inserted into the binding pocket of the substrate glucose and appeared as an overlapped conformation (Fig. 2B). As stated above, the trihydroxybenzene ring was vital for the activity, and it could form strong hydrogen bonds with Asn656, Asp657 and Thr620, thus competing with glucose for the binding site. The hydrazide fragment predicted to form hydrogen bonds with Asp657, Gly681 and Thr680 in the polar pocket, was also preserved in our modifications. Since restriction of rotatable bonds is an effective means of reducing the number of possible spatial conformations and improving target selectivity for small-molecule drugs, the double bond of hydrazine was still retained after further modification. In order to enhance the binding affinity of the lead compounds for HK2, and their pharmacokinetic properties, some appropriate groups were substituted onto the acyl group to improve occupancy of the active binding pocket and their hydrophobicity (Scheme 1).

3.2. Chemistry

The structures and preparation of target compounds (3a–3z) are described in Scheme 1. The esters derived from commercially available acids were selected as starting materials, which were converted into the corresponding hydrazides by reacting with hydrazine hydrate in

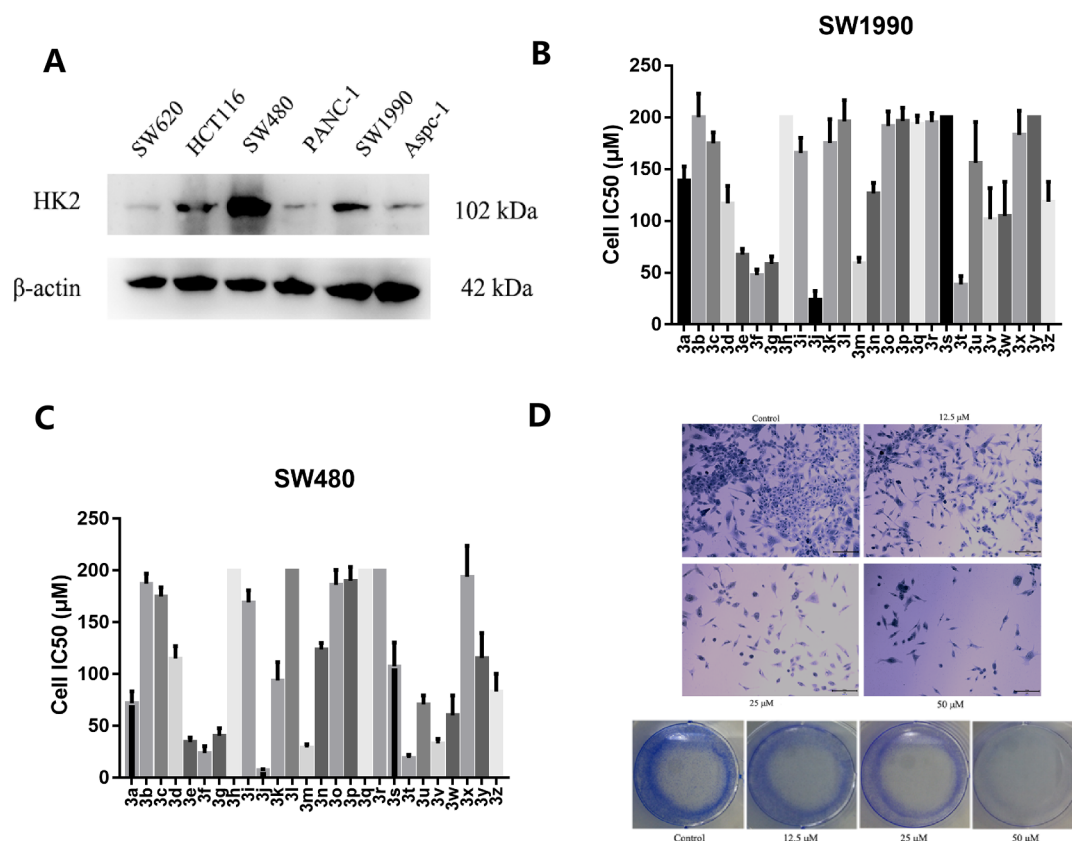


Fig. 4. Compound **3j** inhibits cell proliferation. (A) Western blot analysis of HK2 expression in colon cancer cells and pancreatic cancer cells. (B, C) IC_{50} values of compounds (**3a–3z**) in SW1990 and SW480 cell lines. (D) The colony formation assay of compound **3j** on SW1990 cells.

Table 3

IC_{50} values of designed compounds against two cell lines.

Compounds	Cell IC_{50} (μM)	
	SW1990	SW480
3a	139.00 \pm 13.60	72.00 \pm 11.40
3b	200.00 \pm 23.10	187.10 \pm 9.86
3c	174.80 \pm 10.80	174.80 \pm 8.93
3d	117.00 \pm 16.80	115.00 \pm 11.90
3e	67.30 \pm 5.79	34.50 \pm 4.33
3f	47.50 \pm 5.51	23.80 \pm 6.76
3g	58.40 \pm 7.37	40.60 \pm 7.23
3h	> 200	> 200
3i	165.50 \pm 14.90	169.30 \pm 11.70
3j	24.00 \pm 8.45	7.13 \pm 1.12
3k	175.00 \pm 23.30	93.80 \pm 17.80
3l	196.00 \pm 20.50	> 200
3m	58.80 \pm 5.65	29.30 \pm 3.11
3n	126.50 \pm 10.20	123.80 \pm 6.26
3o	191.60 \pm 14.10	186.10 \pm 14.50
3p	196.30 \pm 12.90	190.20 \pm 13.20
3q	193.60 \pm 7.86	> 200
3r	195.30 \pm 8.74	> 200
3s	> 200	107.50 \pm 23.10
3t	38.60 \pm 8.26	18.76 \pm 3.52
3u	155.90 \pm 39.70	70.65 \pm 8.82
3v	101.60 \pm 30.08	33.29 \pm 4.21
3w	104.70 \pm 33.20	60.39 \pm 19.15
3x	183.00 \pm 23.30	193.90 \pm 30.02
3y	> 200	115.60 \pm 24.10
3z	118.50 \pm 19.30	83.25 \pm 17.11
Metformin	n.p. ^a	n.p.
2-Deoxyglucose	n.p.	n.p.
3-Bromopyruvate	n.p.	n.p.

^a n.p. is not performed.

methanol. Treatment of the latter with 2,3,4-trihydroxybenzaldehyde in anhydrous methanol produced sufficient yields of the desired hydrazone derivatives. Their structures were confirmed by NMR and mass spectrum analyses. The *trans(E)* configuration of the imine double bonds was determined based on the observation that the hydroxyl protons at the *meta*- and *para*-position of imine moiety appeared at δ_H 8.4–9.6, whereas those at the *ortho*-position shifted down-field to δ_H 11.3–12.4 [23,24]. This difference in chemical shift could be explained by the formation of intramolecular hydrogen bonds between the *ortho*-OH group and the N atom of imine when the double bonds were in the *trans(E)* configuration.

3.3. Biological evaluation

3.3.1. Binding affinity and selective inhibition of compound **3j** for the HK2 enzyme

The microscale thermophoresis (MST) technique has been used to assess protein–protein, small molecule–protein, nucleic acid–protein, and antibody–antigen interactions [25–27]. MST was used to assay the binding affinity of the lead compounds (**3a–3z**) for HK2 (Fig. 3A). Among the synthesized compounds, **3j** with an equilibrium dissociation constant (K_d) of $4.99 \pm 0.41 \mu M$ displayed the strongest binding affinity (Fig. 3B, Table 2). The inhibitory activity of the compounds (**3a–3z**) on HK2 enzyme *in vitro* was evaluated by spectrophotometry [28]. Compound **3j** showed the strongest inhibitory effects against HK2 with an IC_{50} value of $0.53 \pm 0.13 \mu M$ (Fig. 3C, Table 2). The molecular docking result of compound **3j** further confirm its same binding mode as the lead zinc03233449 (Fig. 3D).

3.3.2. Compound **3j** inhibits cell proliferation

The protein expression of HK2 by colon cancer and pancreatic cancer cell lines was evaluated *via* western blot analysis. HK2 was

overexpressed in SW480 and SW1990 cell lines (Fig. 4A). The inhibitory effect of compound **3j** on cell proliferation was further examined on SW480 and SW1990 cells. After treatment with compound **3j** for 48 h, the IC₅₀ values of compound **3j** for SW1990 and SW480 cells were 24.0 ± 8.45 μM and 7.13 ± 1.12 μM, respectively (Fig. 4B–C, Table 3). The antiproliferative effect of compound **3j** on SW1990 was also confirmed by colony formation assay (Fig. 4D).

4. Conclusion

In summary, with the aid of structure-based virtual ligand screening, 3 lead compounds with the same active moiety were identified from the ZINC lead-like database. After a careful analysis of their ligand–protein binding mode, we designed a series of novel HK2 inhibitors. These hydrazone derivatives with a *trans(E)* configuration of their imine double bonds were synthesized directly from the corresponding hydrazides and 2,3,4-trihydroxybenzaldehyde. The *trans(E)* configuration is vital to help compounds bind to the pocket in an extended conformation. Substitution by a nitro group at the *para*-position of the benzoyl hydrazine dramatically improved the binding affinity to HK2, which led to the synthesis of compound **3j**. Compound **3j** significantly inhibited cancer cell proliferation by directly targeting HK2. Therefore, compound **3j** is a novel inhibitor of HK2 due to its high activity and deserve further study for future cancer therapeutics.

Declaration of Competing Interest

The authors declare that they have no known competing financial interests or personal relationships that could have appeared to influence the work reported in this paper.

Acknowledgements

We acknowledge support from National Natural Science Foundation of China (NSFC) (grant number Nos. U1803122, 81773637, 81773594, U1703111), National Mega-project for Innovative Drugs (grant number 2019ZX09721001-004-007), and the Fundamental Research Fund for the Central Universities (grant number 2017KFYXJJ151).

Appendix A. Supplementary material

Supplementary data to this article can be found online at <https://doi.org/10.1016/j.bioorg.2020.103609>.

References

- [1] J.W. Kim, C.V. Dang, Cancer's molecular sweet tooth and the Warburg effect, *Cancer Res.* 66 (2006) 8927–8930.
- [2] N.H. Kim, Y.H. Cha, J. Lee, S.H. Lee, J.H. Yang, J.S. Yun, E.S. Cho, X. Zhang, M. Nam, N. Kim, Y.S. Yuk, S.Y. Cha, Y. Lee, J.K. Ryu, S. Park, J.H. Cheong, S.W. Kang, S.Y. Kim, G.S. Hwang, J.I. Yook, H.S. Kim, Snail reprograms glucose metabolism by repressing phosphofructokinase PFKP allowing cancer cell survival under metabolic stress, *Nat. Commun.* 8 (2017) 14374.
- [3] M. Uppara, F. Adaba, A. Askari, S. Clark, G. Hanna, T. Athanasiou, O. Faiz, A systematic review and meta-analysis of the diagnostic accuracy of pyruvate kinase M2 isoenzymatic assay in diagnosing colorectal cancer, *World J. Surg. Oncol.* 13 (2015) 48.
- [4] A. Le, C.R. Cooper, A. Gouw, A. Maitta, R. Dinavahi, L. Deck, R. Royer, D. Vander Jagt, G. Semenza, C. Van Dang, Inhibition of lactate dehydrogenase A induces oxidative stress and inhibits tumor progression, *Proc. Natl. Acad. Sci. U.S.A.* 51 (2010) 1323–1323.
- [5] B. Altenberg, K.O. Greulich, Genes of glycolysis are ubiquitously overexpressed in 24 cancer classes, *Genomics* 84 (2004) 1014–1020.
- [6] K.C. Patra, Q. Wang, P.T. Bhaskar, L. Miller, Z. Wang, W. Wheaton, N. Chandel, M. Laakso, W.J. Muller, E.L. Allen, A.K. Jha, G.A. Smolen, M.F. Clascuin, R.B. Robey, N. Hay, Hexokinase 2 is required for tumor initiation and maintenance and its systemic deletion is therapeutic in mouse models of cancer, *Cancer Cell* 24 (2013) 213–228.
- [7] J.E. Wilson, Isozymes of mammalian hexokinase: structure, subcellular localization and metabolic function, *J. Exp. Biol.* 206 (2003) 2049–2057.
- [8] D.A. Tennant, R.V. Duran, E. Gottlieb, Targeting metabolic transformation for cancer therapy, *Nat. Rev. Cancer* 10 (2010) 267–277.
- [9] W. Guo, Z. Qiu, Z. Wang, Q. Wang, N. Tan, T. Chen, Z. Chen, S. Huang, J. Gu, J. Li, M. Yao, Y. Zhao, X. He, MiR-199a-5p is negatively associated with malignancies and regulates glycolysis and lactate production by targeting hexokinase 2 in liver cancer, *Hepatology* 62 (2015) 1132–1144.
- [10] S. Ros, A. Schulze, Glycolysis back in the limelight: systemic targeting of HK2 blocks tumor growth, *Cancer Discov.* 3 (2013) 1105–1107.
- [11] K.C. Patra, N. Hay, Hexokinase 2 as oncotarget, *Oncotarget* 4 (2013) 1862–1863.
- [12] H. Lin, J. Zeng, R. Xie, M.J. Schulz, R. Tedesco, J. Qu, K.F. Erhard, J.F. Mack, K. Raha, A.R. Rendina, L.M. Szwczuk, P.M. Kratz, A.J. Jurewicz, T. Ceconie, S. Martens, P.J. McDevit, J.D. Martin, S.B. Chen, Y. Jiang, L. Nickels, B.J. Schwartz, A. Smallwood, B. Zhao, N. Campobasso, Y. Qian, J. Briand, C.M. Rominger, C. Oleykowski, M.A. Hardwicke, J.I. Luengo, Discovery of a novel 2,6-disubstituted glucosamine series of potent and selective hexokinase 2 inhibitors, *ACS Med. Chem. Lett.* 7 (2016) 217–222.
- [13] B. Salani, C. Marini, A. Del Rio, S. Ravera, M. Massollo, A.M. Oregno, A. Amaro, M. Passalacqua, S. Maffioli, U. Pfeffer, R. Cordera, D. Maggi, G. Sambucetti, Metformin impairs glucose consumption and survival in Calu-1 cells by direct inhibition of hexokinase-II, *Sci. Rep.* 3 (2013) 2070.
- [14] I. Ben Sahra, K. Laurent, S. Giuliano, F. Larbret, G. Ponzio, P. Gounon, Y. Le Marchand-Brustel, S. Giorgetti-Peraldi, M. Cormont, C. Bertolotto, M. Deckert, P. Auberger, J.F. Tanti, F. Bost, Targeting cancer cell metabolism: the combination of metformin and 2-deoxyglucose induces p53-dependent apoptosis in prostate cancer cells, *Cancer Res.* 70 (2010) 2465–2475.
- [15] W. Kim, J.H. Yoon, J.M. Jeong, G.J. Cheon, T.S. Lee, J.I. Yang, S.C. Park, H.S. Lee, Apoptosis-inducing antitumor efficacy of hexokinase II inhibitor in hepatocellular carcinoma, *Mol. Cancer Ther.* 6 (2007) 2554–2562.
- [16] C. Granchi, D. Fancelli, F. Minutolo, An update on therapeutic opportunities offered by cancer glycolytic metabolism, *ACS Med. Chem. Lett.* 24 (2014) 4915–4925.
- [17] L. Wang, J. Wang, H. Xiong, F. Wu, T. Lan, Y. Zhang, X. Guo, H. Wang, M. Saleem, C. Jiang, J. Lu, Y. Deng, Co-targeting hexokinase 2-mediated Warburg effect and ULK1-dependent autophagy suppresses tumor growth of PTEN- and TP53-deficiency-driven castration-resistant prostate cancer, *Ebiomedicine* 7 (2016) 50–61.
- [18] M. Glick, P. Biddle, J. Jantzi, S. Weaver, D. Schirch, The antitumor agent 3-bromopyruvate has a short half-life at physiological conditions, *Biochem. Biophys. Res. Co.* 452 (2014) 170–173.
- [19] J.J. Hernandez, M. Pryzlak, L. Smith, C. Yanchus, N. Kurji, V.M. Shahani, S.V. Molinski, Giving drugs a second chance: overcoming regulatory and financial hurdles in repurposing approved drugs as cancer therapeutics, *Front. Oncol.* 7 (2017) 273.
- [20] W. Li, M. Zheng, S. Wu, S. Gao, M. Yang, Z. Li, Q. Min, W. Sun, L. Chen, G. Xiang, H. Li, Benserazide, a dopadecarboxylase inhibitor, suppresses tumor growth by targeting hexokinase 2, *Clin. Cancer Res.* 36 (2017) 58–70.
- [21] J.J. Irwin, T. Sterling, M.M. Mysinger, E.S. Bolstad, R.G. Coleman, ZINC: A free tool to discover chemistry for biology, *J. Chem. Inf. Model* 52 (2012) 1757–1768.
- [22] R. Abagyan, M. Totrov, D. Kuznetsov, ICM—A new method for protein modeling and design: Applications to docking and structure prediction from the distorted native conformation, *J. Comput. Chem.* 15 (1993) 488–506.
- [23] H.S. Kareem, A. Ariffin, N. Nordin, T. Heidelberg, A. Abdul-Aziz, K.W. Kong, W.A. Yehye, Correlation of antioxidant activities with theoretical studies for new hydrazone compounds bearing a 3,4,5-trimethoxy benzyl moiety, *Eur. J. Med. Chem.* 103 (2015) 497–505.
- [24] B. Levrard, W. Fieber, J.M. Lehn, A. Herrmann, Controlled release of volatile aldehydes and ketones from dynamic mixtures generated by reversible hydrazone formation, *Helv. Chim. Acta* 90 (2007) 2281–2314.
- [25] S.K. Athuluri-Divakar, R. Vasquez-Del Carpio, K. Dutta, S.J. Baker, S.C. Cosenza, I. Basu, Y.K. Gupta, M.V.R. Reddy, L. Ueno, J.R. Hart, P.K. Vogt, D. Mulholland, C. Guha, A.K. Aggarwal, E.P. Reddy, A Small molecule RAS-mimetic disrupts RAS association with effector proteins to block signaling, *Cell* 165 (2016) 643–655.
- [26] O. De Lange, C. Wolf, J. Dietze, J. Elsaesser, R. Morbitzer, T. Lahaye, Programmable DNA-binding proteins from Burkholderia provide a fresh perspective on the TALE-like repeat domain, *Nucleic Acids Res.* 42 (2014) 7436–7449.
- [27] C.J. Wienken, P. Baaske, U. Rothbauer, D. Braun, S. Dühr, Protein-binding assays in biological liquids using microscale thermophoresis, *Nat. Commun.* 1 (2010) 100.
- [28] F. Bao, K. Yang, C. Wu, S. Gao, P. Wang, L. Chen, H. Li, New natural inhibitors of hexokinase 2 (HK2): steroids from *Ganoderma sinense*, *Fitoterapia* 125 (2018) 123–129.